An entropic Quantum Drift-Diffusion model for electron transport in resonant tunneling diodes

Pierre Degond, Samy Gallego, Florian Méhats

An entropic Quantum Drift-Diffusion model for electron transport in resonant tunneling diodes

Pierre Degond [a], Samy Gallego [a], Florian Méhats [b]

[a] *MIP (UMR CNRS 5640), Université Paul Sabatier, 118 Route de Narbonne, 31062 Toulouse Cedex 4 (France)*

[b] *IRMAR (UMR CNRS 6625), Université de Rennes 1, Campus de Beaulieu, 35042 Rennes Cedex (France)*

Abstract

We present an entropic Quantum Drift Diffusion model (eQDD) and show how it can be derived on a bounded domain as the diffusive approximation of the Quantum Liouville equation with a quantum BGK operator. Some links between this model and other existing models are exhibited, especially with the Density Gradient (DG) model and the Schrödinger-Poisson Drift Diffusion model (SPDD). Then a finite difference scheme is proposed to discretize the eQDD model coupled to the Poisson equation and we show how this scheme can be slightly modified to discretize the other models. Numerical results show that the properties listed for the eQDD model are checked, as well as the model captures important features concerning the modeling of a resonant tunneling diode. To finish, some comparisons between the models stated above are realized.

Key words: entropic Quantum Drift Diffusion, density matrix, Quantum Liouville, Density Gradient, Schrödinger Poisson Drift Diffusion, resonant tunneling diode, current-voltage characteristics

1 Introduction

Miniaturization of semiconductor devices to the nanometer scale increases the role of quantum effects in electron transport. Moreover, new classes of devices operate on the basis of these quantum effects. This is the case for the resonant tunneling diode (RTD) which has attracted and continues to attract interest due to its highly nonlinear static current-voltage characteristic. This device exhibits a negative and non monotonous resistance in a certain range of

applied biases, which is interesting in many applications to logic electronics. The RTD conduction band involves a double potential barrier with one or several resonant energy levels within the well inside the two barriers. Only electrons with energies close to the resonant energy can pass through the double barrier thanks to tunneling effects. Changing the applied bias changes the energy of the incident electrons and increasing the bias can lower the current [10].

The Classical Drift-Diffusion model has been a valuable tool for many years in the semiconductor industry [32] but it is not adapted to the modeling of such devices. In order to capture tunneling effects, one has to use a quantum model. At the microscopic scale, one can use the Schrödinger or the Wigner equation as it is done in [29, 34, 39, 35, 37, 8]. But these models are ballistic quantum models and taking into account collisions in this context is a difficult task. In RTDs, the electron transport in the vicinity of the double barriers can be expected to be quantum and collisionless while transport in the access zone is mainly classical and collisional. This is why a class of hybrid models was developped [1, 13, 9, 27] but the coupling methodology is far from obvious.

An alternative way for modeling quantum effects is by adding quantum corrections terms to classical macroscopic models. The most common quantum correction involves the Bohm potential, which naturally appears in quantum hydrodynamics. In a fluid context, such models were studied in [20, 21, 22, 23, 24, 25, 26]. In a diffusive context, one can find the energy transport model corrected with the Bohm potential [11] and, closer to the eQDD model studied in this paper, the Drift-Diffusion model corrected with the Bohm potential, called Density-Gradient (DG) model (also "Quantum Drift-Diffusion model" in the literature). This model was derived in [6, 5] and studied in [41, 28, 4]. But the Bohm potential has the disadvantage of bringing higher order differential terms which are difficult to handle numerically and mathematically. To conclude this description, one can also cite another recent attempt to include quantum effects in a diffusive model: the Schrödinger-Poisson Drift-Diffusion model (SPDD) derived in [38] and implemented in [12]. This model takes into account the discrete spectrum of energy states for the electrons inside the expression of the density.

In this paper, we propose to use the entropic Quantum Drift-Diffusion (eQDD) model. This model was derived following the moment closure approach developed in [31] and extending it to the context of Quantum mechanics. The strategy consists in defining the notion of "local" quantum equilibrium as the minimizer of an entropy functional under local moment constraints. Such equilibria are defined thanks to a relation between the thermodynamic quantities (such as the chemical potential) and the extensive quantities (density, current,...) in a non local way. In [17], quantum hydrodynamic (QHD) models were derived from the Wigner equation by moment expansions closed by

these quantum equilibria. In this reference, new directions related to these QHD models were sketched, including namely the setting up of a rigorous framework to this formal modeling, the inclusion of other quantum effects (Pauli exclusion principle, spin effects,...), or the numerical discretization and simulation. Following the same approach, a family of ad-hoc collision operators which decrease the quantum entropy and relax to the equilibria were introduced in [16]. Afterwards, this strategy was applied in [14] in order to derive the eQDD model and the Quantum Energy-Transport (QET) model. The eQDD model was written in a more convenient way in the review article [15]. The first attempt to study the model mathematically and numerically was achieved in [18, 19]. The non local relation between the chemical potential and the density makes the model difficult to analyze. The question of the well posedness of the model has not been answered yet but a semidiscretized (in time) version of this model was proposed and rigorously analyzed, as well as a fully discretized version.

The model properties are listed briefly. By construction, the eQDD model takes into account collisions. In [15, 19], we have shown that steady states of this model are solutions of the stationary Schrödinger-Poisson system (studied in [36] for example). Moreover, it is built in order to be consistent with entropy dissipation and the density is always nonnegative (provided the solution exists). Some links were exhibited in [14] between the eQDD model and two other models stated above: the Classical Drift-Diffusion model on the one hand and the Density-Gradient model on the other hand. Indeed, the limit of the eQDD model as the dimensionless Planck constant goes to zero is the Classical Drift-Diffusion model, while the leading order correction term is the Bohm potential.

The aim of this paper is to propose a discretization of the eQDD model on a bounded domain and to check that the above stated properties are numerically verified. We also show that the model can capture the main features of a resonant tunneling diode and compare the eQDD model with the SPDD model and the DG model.

The paper is organized as follows. In section 2, the eQDD model is presented (which is justified in Appendix A by applying formally a diffusive limit to the collisional Quantum Liouville equation). Then links between the eQDD model and the other existing models are briefly given. In section 3, we discretize the models using finite-differences and we perform numerical experiments in section 4. The eQDD model and the SPDD model are compared one to each other on an isolated RTD while the eQDD model and the DG model are compared on a RTD connected to reservoirs, allowing us to compute current-voltage characteristics.

2 Presentation of the models

In this section, we present the entropic Quantum Drift-Diffusion model on a bounded domain (the derivation of this model can be found in appendix A) and we give some links with other existing models. For the sake of readability, parameters like the effective mass, the permittivity and the mobility are supposed constant throughout the device. The reader should refer to appendix B where the models are written with variable parameters.

2.1 The entropic Quantum Drift-Diffusion model (eQDD)

2.1.1 Presentation

In this subsection, the entropic Quantum Drift-Diffusion model is presented on a bounded domain (the boundary conditions will be given in subsection 2.1.3). Let Ω be a regular domain of $\mathbb{R}^d$ ($d = 1, 2$ or 3) . The eQDD model is a quantum fluid model describing the evolution of the electron density $n(t, x)$ subject to the electrical potential $V(t, x)$ and interacting with a thermal bath of fixed temperature T. The first equation is the equation of mass conservation and reads:

$$e\partial_t n - \mathrm{div} j = 0, \tag{1}$$

where e is the positive electron charge and j is the current defined as follows:

$$j = e\mu n \nabla(A - V). \tag{2}$$

In this equation, μ is the electron mobility. We call $A(t, x)$ the quantum chemical potential which is linked to the density of electrons by a relation which is non local in space and which is the key of this quantum model:

$$n[A] = \sum_{p\geq 1} \exp(-\frac{\lambda_p[A]}{k_B T})|\psi_p[A]|^2. \tag{3}$$

Here k_B is the Boltzmann constant and $(\lambda_p, \psi_p)_{p\geq 1}$ are the eigenvalues and the normalized eigenfunctions of the following modified Hamiltonian (where the electrical potential is replaced by the quantum chemical potential):

$$H[A] = -\frac{\hbar^2}{2m}\Delta - eA, \tag{4}$$

where $\hbar$ is the Planck constant and m is the effective mass of an electron.

The electrical potential V can be split into a given external potential V_{ext} (assumed independent of time for simplicity) and a self consistent potential

V_s created by the difference between a given doping density C and the electron density n according to the following Poisson equation:

$$-\varepsilon \Delta V_s = e(C - n), \tag{5}$$

where ε is the permittivity of the semiconductor.

2.1.2 Scaling

Before introducing the other models, it is useful to rewrite the eQDD model in a scaled form. We take for reference density $\overline{n}$, the maximum value of the doping profile throughout the device: $\overline{n} = \max |C|$. We assume that the device has a characteristic length $\overline{x} = L$ and voltages are scaled with respect to the thermal potential: $\overline{V} = \frac{k_B T}{e}$. Finally, we take the following reference values for the time and the current: $\overline{t} = \frac{L^2 e}{\mu k_B T}$ and $\overline{j} = \frac{\mu k_B T \overline{n}}{Le}$. Then we write the following dimensionless quantities:

$$n' = \frac{n}{\overline{n}} \; ; \; x' = \frac{x}{\overline{x}} \; ; \; j' = -\frac{j}{\overline{j}} \; ; \; t' = \frac{t}{\overline{t}} \; ; \; V' = -\frac{V}{\overline{V}} \; ; \; A' = -\frac{A}{\overline{V}} + \log \overline{n} \; ;$$

and obtain the eQDD model coupled with the Poisson equation (forgetting the primes):

$$\partial_t n + \mathrm{div} j = 0, \tag{6}$$
$$j = n \nabla (A - (V_s + V_{ext})), \tag{7}$$
$$-\alpha^2 \Delta V_s = n - C, \tag{8}$$
$$n = \sum_{p \geq 1} e^{-\lambda_p[A]} |\psi_p[A]|^2, \tag{9}$$

where $(\lambda_p[A], \psi_p[A])$ are the eigenvalues and eigenfunctions of the Hamiltonian

$$H[A] = -\beta^2 \Delta + A,$$

α and β being the scaled Debye length and the scaled de Broglie length:

$$\alpha = \sqrt{\frac{\varepsilon k_B T}{e^2 L^2 \overline{n}}} = \frac{\lambda_D}{L}, \tag{10}$$
$$\beta = \sqrt{\frac{\hbar^2}{2mL^2 k_B T}} = \frac{\lambda_{dB}}{L}. \tag{11}$$

2.1.3 Boundary conditions

Boundary conditions for the wave functions. We have chosen for the wave functions Neumann boundary conditions permitting to define a density which does not vanish on the boundary as we need to allow a current flow to exist:

$$\forall p \geq 1 \quad \nabla \psi_p \cdot \nu = 0 \quad \text{on } \partial\Omega, \tag{12}$$

where the boundary is denoted by $\partial\Omega$ and $\nu(x)$ is the outward unit normal vector at $x \in \partial\Omega$.

Boundary conditions for the potentials. In this work, two classes of boundary conditions will be studied:

- Insulating boundary conditions. The total number of particles in the domain is enforced to be constant by putting Neumann boundary conditions on the electrochemical potential (and thus the current vanishes on the boundary):

  $$\nabla(A - (V_s + V_{ext})) \cdot \nu = 0 \quad \text{on } \partial\Omega.$$

  Moreover, no bias is applied on the device, which is translated by the following Dirichlet conditions on the electrical potential:

  $$V_s = 0 \quad \text{on } \partial\Omega.$$

- Open boundary conditions. In order to allow a current flow at the boundary, non homogeneous Dirichlet conditions are applied on the density:

  $$n = \sum_{p \geq 1} e^{-\lambda_p[A]} |\psi_p[A]|^2 = C \quad \text{on } \partial\Omega,$$

  and non homogeneous Dirichlet conditions on the electrical potential V_s:

  $$V_s = V_0 \quad \text{on } \partial\Omega.$$

  The function $V_0(x)$ permits to control the bias applied on the device.

2.1.4 Properties of the isolated system

Entropy dissipation. An important property of the eQDD model coupled to the Poisson equation is that, if we choose boundary conditions isolating the domain Ω, the macroscopic quantum free energy G defined by

$$G = \int_\Omega -n(A - V_{ext}) + \frac{\alpha^2}{2} |\nabla V_s|^2 \, dx$$

is a decreasing function of time:

$$\frac{d}{dt} G = -\int_\Omega n |\nabla(A - (V_s + V_{ext}))|^2 \, dx \ \leq \ 0.$$

This property is a consequence of the method of the model derivation (see appendix A) where the density matrix is chosen to minimize the microscopic quantum free energy and thus the system is at any time in a local equilibrium.

Steady states. Another interesting property of the eQDD model with insulating boundary conditions is that steady states are solutions of the Schrödinger-Poisson model (SP). Let (n, A, V_s) be a steady state of (6)-(9) such that $\int_\Omega n(x)dx = N$, then there exists a constant ϵ_F (the quantum quasi Fermi level) such that $A - (V_s + V_{ext}) = \epsilon_F$ and (n, V_s, ϵ_F) is the unique solution of the Schrödinger-Poisson model under a constraint of total charge:

$$-\alpha^2 \Delta V_s = n - C, \tag{13}$$
$$n = \sum_{p \geq 1} e^{\epsilon_F - \lambda_p} |\psi_p|^2, \tag{14}$$
$$\int_\Omega n(x)dx = N, \tag{15}$$

where (λ_p, ψ_p) are the eigenvalues and the normalized eigenfunctions of the Hamiltonian: $\mathcal{H} = H[V_s + V_{ext}] = -\beta^2 \Delta + (V_s + V_{ext})$.

2.2 Links with other existing models

2.2.1 The Classical Drift-Diffusion model (CDD)

Presentation. We are going to present now the classical counterpart of the eQDD model. The CDD model coupled to the Poisson equation can be written with the same dimensionless parameter α and is independent of the scaled Planck constant β:

$$\partial_t n + \mathrm{div} j = 0, \tag{16}$$
$$j = n\nabla(-\log n - (V_s + V_{ext})), \tag{17}$$
$$-\alpha^2 \Delta V_s = n - C. \tag{18}$$

The term $n\nabla \log n = \nabla n$ is the diffusion term of the current and $n\nabla(V_s + V_{ext})$ is the drift term. The same boundary conditions as for the eQDD model can be used: Neumann conditions on $-\log n - (V_s + V_{ext})$ permit to isolate the device while Dirichlet conditions on the density n allow a current at the boundary (the conditions for the electrical potential are unchanged).

Link with the eQDD model. In order to display a link between the eQDD model (6)-(9) and the CDD model (16)-(18), it is possible to expand the

density for the eQDD model (9) in powers of the scaled Planck constant β (see [14]). Let A be a smooth function of x, then:

$$n[A] = \sum_{p\geq 1} e^{-\lambda_p[A]}|\psi_p[A]|^2 = n_0 e^{-A} + \mathcal{O}(\beta^2), \tag{19}$$

where $n_0 = (4\pi\beta^2)^{d/2}$ is the effective density of states. This gives:

$$A = -\log n + \log n_0 + \mathcal{O}(\beta^2). \tag{20}$$

Putting this relation in (7), we find the expression of the current for the CDD model (17). The difference between the eQDD model and the CDD model being of order β^2, we will note formally:

$$\text{eQDD} - \text{CDD} = \mathcal{O}(\beta^2).$$

2.2.2 The Density Gradient model (DG)

Presentation. The difference between the DG model and the CDD model lies in a term of order β^2 (called the Bohm potential) that is added in the current expression (only equation (17) changes and is replaced by equation (22)):

$$\partial_t n + \text{div} j = 0, \tag{21}$$
$$j = n\nabla(-\log n - (V_s + V_{ext} + V_B)), \tag{22}$$
$$-\alpha^2 \Delta V_s = n - C, \tag{23}$$
$$V_B = -\frac{\beta^2}{3}\frac{\Delta\sqrt{n}}{\sqrt{n}}. \tag{24}$$

Since this is a fourth order parabolic system, we need an additional boundary condition. The most standard choice consists in an homogeneous Dirichlet conditions on the Bohm potential, assuming there is no quantum effect on the boundary (see [28]):

$$V_B = 0 \ \text{ on } \partial\Omega. \tag{25}$$

Link with the eQDD model. We want to show a link between the eQDD model (6)-(9) and the DG model (21)-(24). If the terms of order β^2 are explicitely written in the expansion (19), one obtains:

$$n[A] = \sum_{p\geq 1} e^{-\lambda_p[A]}|\psi_p[A]|^2 = n_0 e^{-A}\left(1 + \frac{\beta^2}{12}(-2\Delta A + |\nabla A|^2)\right) + \mathcal{O}(\beta^4). \tag{26}$$

Using relation (20), it follows:

$$A = -\log n + \log n_0 + \frac{\beta^2}{3}\frac{\Delta\sqrt{n}}{\sqrt{n}} + \mathcal{O}(\beta^4). \tag{27}$$

Putting this relation in (7), we find the expression of the current for the DG model (22).

The difference between the eQDD model and the DG model being of order β^4, we will note formally:

$$\text{eQDD} - \text{DG} = \mathcal{O}(\beta^4).$$

2.2.3 The Schrödinger-Poisson Drift-Diffusion model (SPDD)

Presentation: The simplified version of the Schrödinger-Poisson Drift-Diffusion model introduced in [38] is very close to the eQDD model, except that the expression of the density is different. In the SPDD model, electron density can be expressed as:

$$n(x) = \int_0^\infty g(\epsilon) e^{-A-\epsilon}\, d\epsilon, \tag{28}$$

where $g(\epsilon)$ is the density of states corresponding to the energy ϵ. In a classical model, we would have $g(\epsilon) = \frac{2}{\sqrt{\pi}} n_0 \sqrt{\epsilon}$ while in the SPDD model, we have:

$$g(\epsilon) = \sum_{p\geq 1} \delta(\epsilon - \lambda_p[V_s + V_{ext}] + (V_s + V_{ext}))\ |\psi_p[V_s + V_{ext}]|^2,$$

where δ is the Dirac delta function and $\lambda_p[V_s + V_{ext}]$ and $\psi_p[V_s + V_{ext}]$ are the eigen elements of the Hamiltonian $\mathcal{H} = H[V_s + V_{ext}] = -\beta^2\Delta + (V_s + V_{ext})$. This gives the following system (only equation (9) changes in the eQDD model and is replaced by (32)):

$$\partial_t n + \text{div} j = 0, \tag{29}$$
$$j = n\nabla(A - (V_s + V_{ext})), \tag{30}$$
$$-\alpha^2 \Delta V_s = n - C, \tag{31}$$
$$n = \sum_{p\geq 1} e^{-\lambda_p - A + (V_s + V_{ext})} |\psi_p|^2. \tag{32}$$

Link with the eQDD model. Both models can be linked in the case where we take insulating boundary conditions. The SPDD model can then be seen as an intermediate model between the eQDD model and the stationary Schrödinger-Poisson system (13)-(15) in a situation close to the equilibrium.

Indeed, if the current $j = n\nabla(A-V)$ is small, this means that the electrochemical potential $\varphi(x) = A(x) - V(x)$ is slowly variable. Then the commutator between the Hamiltonian $\mathcal{H} = H[V] = -\beta^2\Delta + V$ and $\varphi(x)$ is small and a "space-adiabatic" approximation can be performed in the expression of the density given by the eQDD model:

$$\begin{aligned} n^{\mathrm{eQDD}} &= \sum_{p\geq 1} e^{-\lambda_p[V+\varphi]}|\psi_p[V+\varphi]|^2 \\ &\sim \sum_{p\geq 1} e^{-\lambda_p[V]-\varphi}|\psi_p[V]|^2 = n^{\mathrm{SPDD}}. \end{aligned}$$

For a discussion on space adiabatic approximation in the context of Born-Oppenheimer approximation in molecular dynamics, one can refer for instance to [40].

2.2.4 Summary

We can summarize the links between the eQDD model and the other models with the following diagram:

$$\begin{array}{ccccc} & & \textit{(Semiclassical limit)} & & \\ & & \mathrm{eQDD} & \longrightarrow \ \mathrm{DG} \ \longrightarrow & \mathrm{CDD} \\ & & \downarrow & & \\ \textit{(Convergence to the equilibrium)} & & \mathrm{SPDD} & & \\ & & \downarrow & & \\ & & \mathrm{SP} & & \end{array}$$

3 Numerical Methods

3.1 Numerical scheme for the eQDD model

The space dimension is now $d = 1$ so that the domain Ω is $(0, 1)$. Parameters such as the mobility, the permittivity and the effective mass are now variable (the reader should refer to appendix B where the models are written with variable parameters). The eQDD model is discretized in time using a semi implicit Euler scheme in order to preserve the quantum free energy dissipation. We discretize the space variable using finite-differences. Let $\Delta t > 0$ be the time step and $\Delta x = \frac{1}{N+1}$ the space gridstep. The grid is composed of the points

$x_i = i\Delta x$ for $i = 0 \cdots N+1$, where $N \in \mathbb{N}$. The unknowns are the chemical potential A_i^k and the self consistent electrical potential $V_{s,i}^k$ at the point x_i and at the time $t_k = k\Delta t$. For the sake of readability, we use the auxiliary variables n_i^k for the density and j_i^k for the current.

The fully discretized scheme for the eQDD model coupled to the Poisson equation reads for $i = 1 \cdots N$:

$$\frac{n_i^{k+1} - n_i^k}{\Delta t} + \frac{j_i^{k+1} - j_{i-1}^{k+1}}{\Delta x} = 0, \tag{33}$$

$$j_i^{k+1} = \mu_i n_i^k \frac{(A_{i+1}^{k+1} - (V_{ext,i+1} + V_{s,i+1}^{k+1})) - (A_i^{k+1} - (V_{ext,i} + V_{s,i}^{k+1}))}{\Delta x}, \tag{34}$$

$$-\frac{\alpha^2}{\Delta x^2}(\varepsilon_i(V_{s,i+1}^{k+1} - V_{s,i}^{k+1}) - \varepsilon_{i-1}(V_{s,i}^{k+1} - V_{s,i-1}^{k+1})) = n_i^{k+1} - C_i, \tag{35}$$

$$n_i^{k+1} = \sum_{p \geq 1} \exp(-\lambda_p[A^{k+1}])|\psi_{p,i}[A^{k+1}]|^2, \tag{36}$$

where $(\lambda_p[A^{k+1}], \psi_p[A^{k+1}])_{p\geq 1}$ is the whole sequence of eigenvalues and eigenvectors of the $(N+2) \times (N+2)$ tridiagonal matrix H^{k+1} discretizing the modified Hamiltonian $H[A(t_{k+1}, x)]$. This tridiagonal matrix H^{k+1} is defined by (for $i = 1 \cdots N$):

$$\begin{aligned}
H_{i,i-1}^{k+1} &= -\frac{\beta^2}{\Delta x^2}\frac{1}{m_i}, \\
H_{i,i}^{k+1} &= \frac{\beta^2}{\Delta x^2}(\frac{1}{m_{i+1}} + \frac{1}{m_i}) + A_i^{k+1}, \\
H_{i,i+1}^{k+1} &= -\frac{\beta^2}{\Delta x^2}\frac{1}{m_{i+1}},
\end{aligned}$$

and the other components $H_{i,j}^{k+1}$ with $j \notin \{i-1, i, i+1\}$ are zero. For each i, the vector component m_i of the effective mass is defined by:

$$m_i = \frac{1}{\Delta x}\int_{x_{i-1/2}}^{x_{i+1/2}} m(x)dx$$

The vectors defining the mobility of the electrons (μ), the permittivity of the semiconductor (ε) as well as the doping profile (C) are calculated in the same way.

Boundary conditions. The Neumann conditions on the eigenfunctions ψ give for the matrix H:

$$H_{0,0}^{k+1} = \frac{\beta^2}{\Delta x^2}\frac{1}{m_0} + A_0^{k+1}\,, H_{0,1}^{k+1} = -\frac{\beta^2}{\Delta x^2}\frac{1}{m_1},$$
$$H_{N+1,N}^{k+1} = -\frac{\beta^2}{\Delta x^2}\frac{1}{m_N}\,, H_{N+1,N+1}^{k+1} = \frac{\beta^2}{\Delta x^2}\frac{1}{m_{N+1}} + A_{N+1}^{k+1}.$$

In order to complete the scheme, we prescribe boundary conditions on the potentials:

- Insulating boundary conditions: We put homogeneous Dirichlet conditions on the electrical potential V_s:

  $$V_{s,0} = 0 \quad ; \quad V_{s,N+1} = 0.$$

  The Neumann conditions on the electrochemical potential give:

  $$(A_1^{k+1} - (V_{ext,1} + V_{s,1}^{k+1})) - (A_0^{k+1} - (V_{ext,0} + V_{s,0}^{k+1})) = 0,$$
  $$(A_{N+1}^{k+1} - (V_{ext,N+1} + V_{s,N+1}^{k+1})) - (A_N^{k+1} - (V_{ext,N} + V_{s,N}^{k+1})) = 0.$$

- Open boundary conditions: We prescribe non homogeneous Dirichlet conditions on the electrical potential, V_r being the parameter permitting to control the applied bias:

  $$V_{s,0} = 0 \quad ; \quad V_{s,N+1} = V_r.$$

  The non homogeneous Dirichlet conditions on the density give:

  $$n_0^{k+1} = \sum_{p\geq 1} e^{-\lambda_p[A^{k+1}]}|\psi_{p,0}[A^{k+1}]| = C_0;$$
  $$n_{N+1}^{k+1} = \sum_{p\geq 1} e^{-\lambda_p[A^{k+1}]}|\psi_{p,N+1}[A^{k+1}]| = C_{N+1}.$$

Algorithm. Given an initial positive density n^0 we solve the scheme for each time step using Newton algorithm implemented with Matlab. It is well known that the efficiency of the Newton method depends on the initial guess of the variables. For all time steps $k \geq 2$, it is natural to initialize the electrical potential with V_s^{k-1} and the chemical potential with A^{k-1}. For the first time step, it is easy to solve the Poisson equation to find the electrical potential V_s^0 corresponding to the density n^0 and thus we have a good initial guess. It is a little bit more difficult to initialize the chemical potential A^0. We have proved in [19] the existence and uniqueness of the quantum chemical potential A^0 corresponding to n^0. It has been shown to be the solution of a minimization problem which is easy to implement. Nevertheless, when β is very small (high temperature), we can also initialize A by considering the semiclassical limit $n \approx \frac{\sqrt{m}}{2\beta\sqrt{\pi}}e^{-A}$, giving $A^0 = -\log n^0 + \frac{1}{2}\log m - \log 2\beta\sqrt{\pi}$. On the contrary, if β is large, we can consider the limit (near the zero temperature) where the

expression of the density is given by $n \approx e^{-\lambda_1}|\psi_1|^2$. This gives (we recognize the Bohm potential appearing with a factor 3) $A^0 = -\log\left(\int_\Omega n^0\ dx\right) + \beta^2 \frac{\partial_x^2 \sqrt{n^0}}{\sqrt{n^0}}$.

Note that we have to solve an eigenvalue problem for each Newton iteration which is numerically expensive (we use the Matlab function `eigs`). Hopefully, the dependence on the eigenvalues is exponential and we need only the few lowest ones. In fact, (36) is replaced by:

$$n_i^{k+1} = \sum_{p=1}^{p_{\max}} \exp(-\lambda_p[A^{k+1}])|\psi_{p,i}[A^{k+1}]|^2.$$

The value of $p_{\max}$ is chosen such that $N \exp(-\lambda_{p_{\max}})$ is below a small given tolerance value; note that for this prediction we use the asymptotic formula: $\lambda_p \sim \beta^2 p^2 \pi^2$ (valid for large p's).

3.2 Numerical schemes for the other models

The DG and CDD schemes. For the discretization of the DG and CDD model, we employ an exponential change of variable which permits to define a scheme very similar to the one of the eQDD model. Let us note $n = e^{-u}$, so that we can rewrite the DG model as follows (here, we still assume that m, ε and μ are independent of x for simplicity):

$$\begin{aligned}
&\partial_t n + \mathrm{div} j = 0,\\
&j = n\nabla(u - (V_s + V_{ext} + V^B)),\\
&-\alpha^2 \Delta V_s = n - C,\\
&V_B = -\frac{\beta^2}{12}(-2\Delta u + |\nabla u|^2),\\
&n = e^{-u}.
\end{aligned}$$

Now the unknowns for the scheme are the u_i^k and $V_{s,i}^k$ at the point x_i and at the time $t_k = k\Delta t$. The scheme reads for $i = 1 \cdots N$:

$$
\begin{aligned}
&\frac{n_i^{k+1}-n_i^k}{\Delta t}+\frac{j_i^{k+1}-j_{i-1}^{k+1}}{\Delta x}=0,\\
&j_i^{k+1}=\mu_i n_i^k\frac{(u_{i+1}^{k+1}-(V_{ext,i+1}+V_{s,i+1}^{k+1}))-(u_i^{k+1}-(V_{ext,i}+V_{s,i}^{k+1}))}{\Delta x},\\
&-\frac{\alpha^2}{\Delta x^2}(\varepsilon_i(V_{s,i+1}^{k+1}-V_{s,i}^{k+1})-\varepsilon_{i-1}(V_{s,i}^{k+1}-V_{s,i-1}^{k+1}))=n_i^{k+1}-C_i,\\
&n_i^{k+1}=e^{-u_i^{k+1}}\\
&V_{B,i}^k=-\frac{\beta^2}{12\Delta x^2}\left(-\frac{2}{m_i}(u_{i+1}^k-u_i^k)+\frac{2}{m_{i-1}}(u_i^k-u_{i-1}^k)+\frac{1}{m_i}\left|u_{i+1}^k-u_i^k\right|^2\right).
\end{aligned}
$$

The boundary conditions can be easily deduced from the one applied for the eQDD scheme and we add homogenous Dirichlet conditions on the Bohm potential (see subsection 2.2.2):

$$V_{B,0}=V_{B,N+1}=0. \tag{37}$$

For the CDD model, we use the same scheme but $V_{B,i}=0$ for $i=0\cdots N+1$.

Remark that fixing the density on the boundary (in the case of open boundary conditions) automatically fixes the unknown u_i^k on the boundary. For the eQDD model, the relation between the quantum chemical potential A and the density n being non local, the unknown A is not a priori fixed on the boundary.

The SPDD scheme. For the SPDD model, the only difference with the scheme for the eQDD model lies in the expressions of the density and the Hamiltonian which are modified in consequence:

$$n_i^{k+1}=\sum_{p\geq 1}\exp(-\lambda_p[V_s^{k+1}+V_{ext}]-A_i^{k+1}+V_{s,i}^{k+1}+V_{ext,i})\ |\psi_{p,i}[V_s^{k+1}+V_{ext}]|^2,$$

where $(\lambda_p[V_s^{k+1}+V_{ext}],\psi_p[V_s^{k+1}+V_{ext}])$ are the eigen elements of the tridiagonal matrix $\mathcal{H}^{k+1}$ defined by (for $i=1\cdots N$):

$$
\begin{aligned}
\mathcal{H}_{i,i-1}^{k+1}&=-\frac{\beta^2}{\Delta x^2}\frac{1}{m_i},\\
\mathcal{H}_{i,i}^{k+1}&=\frac{\beta^2}{\Delta x^2}(\frac{1}{m_{i+1}}+\frac{1}{m_i})+V_{s,i}^{k+1}+V_{ext,i},\\
\mathcal{H}_{i,i+1}^{k+1}&=-\frac{\beta^2}{\Delta x^2}\frac{1}{m_{i+1}}.
\end{aligned}
$$

To complete the scheme, we add boundary conditions that can be easily deduced from the one applied for the eQDD scheme. All the schemes are solved using the Newton algorithm.

4 Numerical results

Our aim is to check the properties stated for the eQDD model in the two kinds of situations: with insulating or open boundary conditions. We also want to compare the eQDD model with the SPDD model and the DG model. For the numerical investigations, the devices that we have chosen are resonant tunneling diodes (RTD). For the use of the open boundary conditions, the structure of the studied RTD is depicted in figure 1. It consists of two 5nm barriers of $Al_{0.3}Ga_{0.7}As$ separated by a 5nm well of $GaAs$. The double barrier is sandwiched between two 5nm spacer layers and two 25nm $GaAs$ highly doped access zones (doping density equal to $10^{24}m^{-3}$), while the channel is moderately doped (doping density eqal to $10^{21}m^{-3}$). For the use of the insulating boundary conditions, the RTD is chosen with a doping profile equal to 0. The schemes which have been developped in the previous sections have been implemented in Matlab and the time and space steps are taken equal to 5×10^{-3} in the dimensionless units.

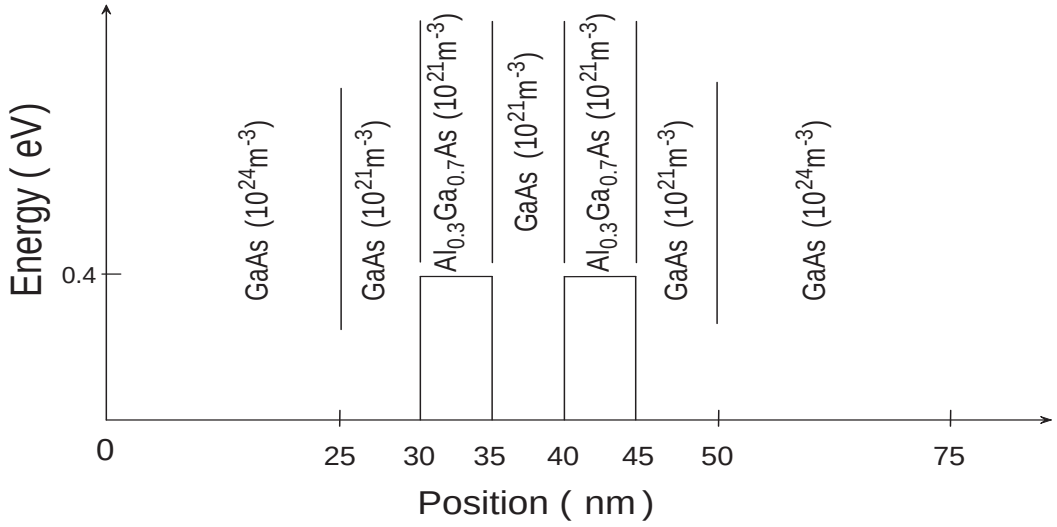

Fig. 1. The double barrier resonant tunneling structure.

4.1 Insulating boundary conditions

4.1.1 The eQDD model

The parameters are all chosen independant of x in this case and are given in table 1. The corresponding dimensionless parameters have values equal to $\alpha = 1.7061$ and $\beta = 0.0625$. The initial density is concentrated to the left of the double barrier and figure 2 shows the evolution of electrons for the eQDD model under insulating boundary conditions. Steady state is achieved at about $6000fs$ as confirmed by the next figure (figure 3) which demonstrates that the

quantum free energy is no more evolving (the figure shows also clearly that the quantum free energy is a decreasing function of time). Figure 4 displays the evolution of the electrochemical potential $\varphi(x) = A(x) - (V_s(x) + V_{ext}(x))$ and we can see that it is constant at $t = 10000\ fs$ (and equal to $0.0623V$). At equilibrium, the density (which is a solution of the Schrödinger-Poisson (SP) model) is perfectly symmetric and the mass has been conserved up to a relative error of $10^{-4}\%$.

effective mass $m(kg)$	mobility $\mu(m^2V^{-1}s^{-1})$	permittivity $\varepsilon(Fm^{-1})$	temperature T(K)
$0.067 \times 9.11e-31$	0.85	$11.44 \times 8.85e-12$	300

Table 1
Parameters used for the modeling of an isolated RTD.

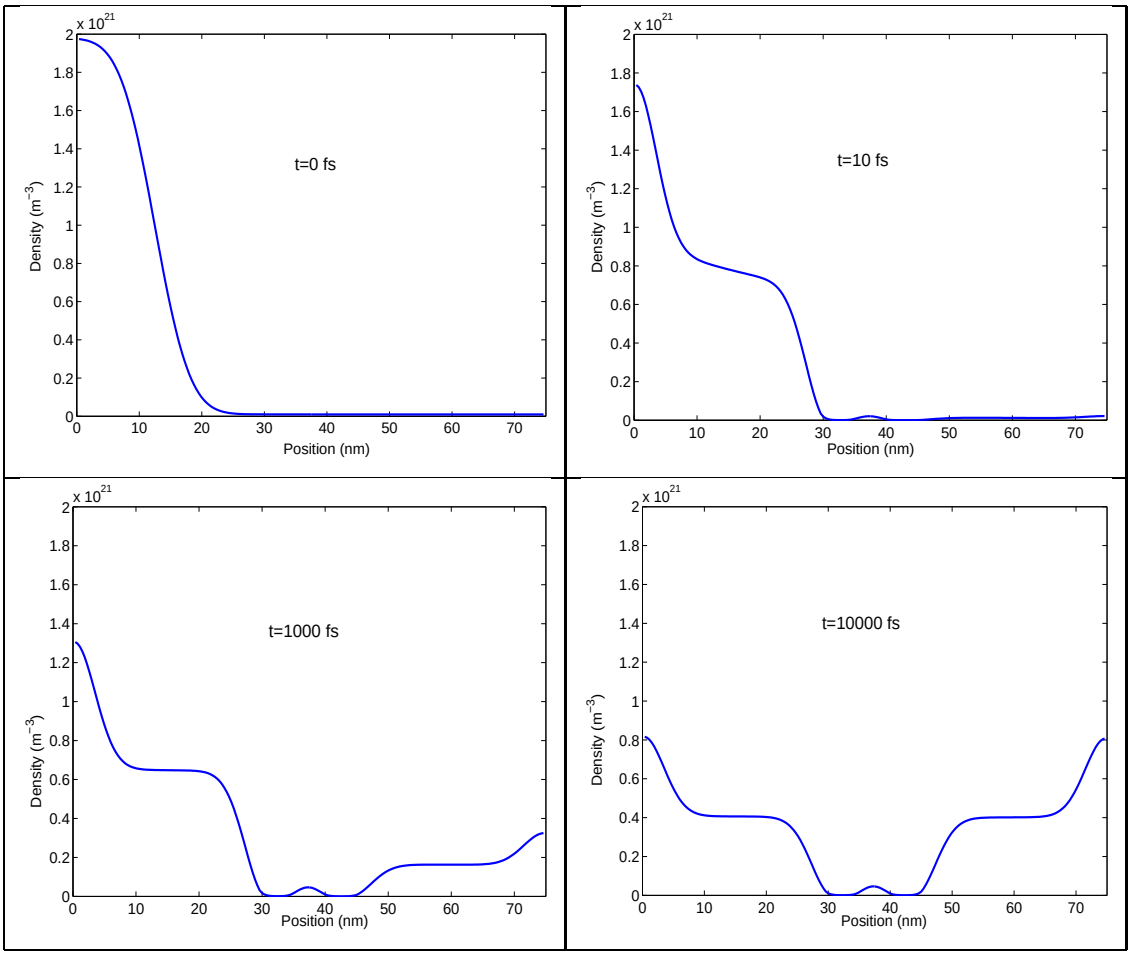

Fig. 2. Electron density at different times ($t = 0, 10, 1000$ and $10000\ fs$) for the eQDD model.

4.1.2 Comparison between the eQDD model and the SPDD model

Figure 5 permits to compare the eQDD model, the SPDD model and the stationary SP model. The dashed line shows the evolution of the relative

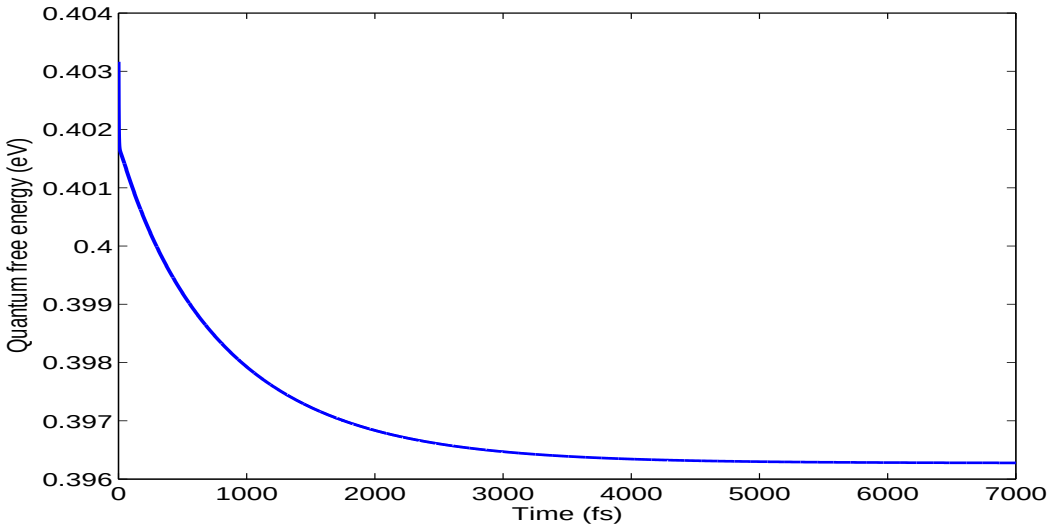

Fig. 3. Evolution of the Quantum free energy.

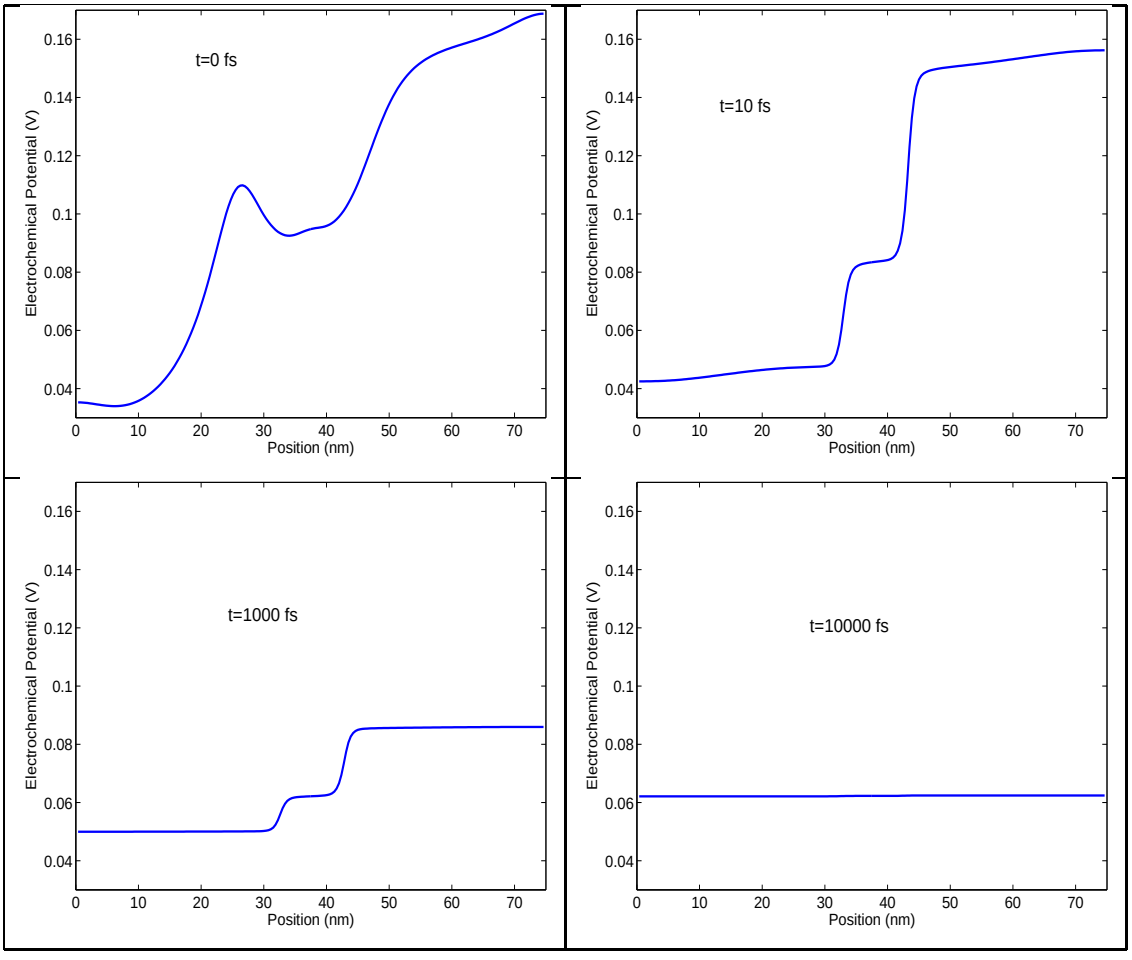

Fig. 4. Electrochemical potential ($\varphi(x) = A - (V_s + V_{ext})$) at different times ($t = 0, 10, 1000$ and $10000\ fs$).

difference (in L^2 norm) between the densities for the eQDD model and the SPDD model while the solid line shows the evolution of the relative difference between the densities for the eQDD model and the SP model. The eQDD and the SPDD model are closer than the eQDD and the SP models (as suggested in section 2.2) but the relative difference between the densities decreases with the same rate.

The eQDD model and the SPDD model with insulating boundary conditions seem very close but if we apply open boundary conditions and if the applied bias is too high, it appears that the SPDD model is not as stable as the eQDD model. The current oscillates and does not stabilize. This is why we have not been able to plot current-voltage characteristics for the SPDD model. This is perhaps due to the fact that the SPDD model is not entropic. However, we have been able to compare IV curves for the eQDD model and the DG model (see next section).

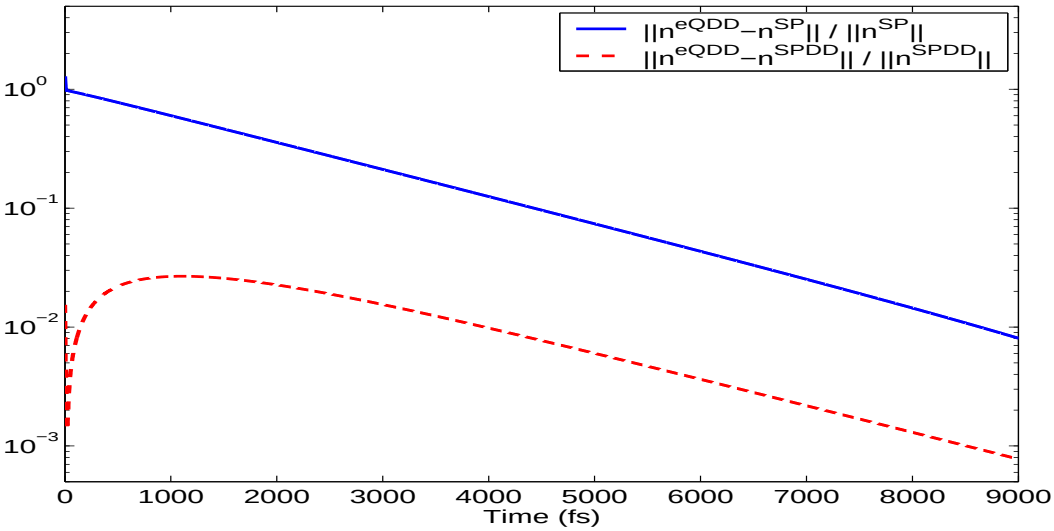

Fig. 5. Comparison between the eQDD model and the SPDD model (dashed line), and between the eQDD model and the SP model (solid line).

4.2 Open boundary conditions

4.2.1 The eQDD model

The goal of this subsection is to check if the eQDD model captures some properties of a RTD and to analyse the influence of the effective mass on the current-voltage characteristics. For each bias V_r applied on the diode, we find the stationary state and we record the corresponding current $j(V_r)$. We consider that the stationary state is achieved when $\frac{\max(j)-\min(j)}{\text{mean}(j)} \leq 10^{-2}$ (this constant was fixed heuristically).

Let us first analyze the influence of the effective mass on the shape of the IV curve. The temperature is chosen equal to $77K$ and the mobility is supposed to be constant and equal to $0.85\ m^2V^{-1}s^{-1}$. The permittivity is also supposed to be constant and equal to $11.44\ \varepsilon_0$. Figure 6 shows four different IV curves with different values of the effective mass inside and outside the double barriers. As pointed out in [33], this parameter appears to be critical to obtain resonance with the DG model and it seems to be the same for the eQDD model. To be more precise, an interesting feature that can be seen on figure 6 is that the IV curve is much more sensitive on m_2 (the effective mass inside the AlGaAs barriers) than on m_1 (the effective mass in the GaAs, outside the barriers). Note that with the most realistic physical values ($m_1 = 0.067m_e$ and $m_2 = 0.092m_e$), the IV curve does not show negative resistance and we need to artificially increase the effective masses to see such phenomenon appear (this was also done for the DG model in [33, 41]). An explanation to this phenomenon could be that the approximation of effective mass is unappropriate for small distances (one barrier is only 50Å long). We can also see that as expected, increasing the effective mass lowers the current.

Figure 7 shows the time evolution of the density from the peak to the valley when the effective mass is $m_2 = 1.5 \times 0.092m_e$ inside the barriers and $m_1 = 1.5 \times 0.067m_e$ outside it (corresponding to the IV curve at the bottom right of figure 6). To obtain this figure, we apply a voltage of $0.25V$ and wait for the electrons to achieve the stationary state. Then we suddenly change the value of the applied bias to $0.29V$ and we record the evolution of the density. As expected, the density inside the well grows significantly and the stationary state is achieved at about $1500fs$.

A small density depletion can be observed on the edge, which does not seems physical. It may be due to the choice in our model of Neumann boundary conditions for the wave functions whereas open (or transparent) boundary conditions should be preferable. However, because this "boundary layer" appears inside the doped region, it does not seem to affect the current, but this question requires more investigations.

The next two figures (fig. 8 and fig. 9) display the details of the reconstruction of the density from the eigenstates ψ_p (for $p = 1 \cdots 6$) of the modified Hamiltonian $H[A]$. The density $e^{-\lambda_p}|\psi_p|^2$ corresponding to each eigenstate is plotted for two values of the applied bias, respectively corresponding to the current peak (fig.8) and to the valley (fig.9). Table 4.2.1 shows the values of the corresponding energies λ_p. Some interesting features can be pointed out. First, the eigenstates split in three categories: three of them ($p = 1, 3, 6$) correspond to wave functions which give rise to the density of incident electrons (on the left hand side of the double barrier), one and only one ($p = 4$) describes the electrons inside the well and two wavefunctions ($p = 2, 5$) correspond to electrons on the right hand side of the double barrier. Table 4.2.1 shows

clearly that the voltage shift has no incidence on the energies corresponding to the incident electrons while the energies of the electrons on the right hand side of the double barriers increase. An important change concerns the energy corresponding to electrons which are trapped inside the well, starting with an energy of $2.03eV$ and finishing with an energy of $1.70eV$, explaining the density increase in this region.

Lastly, figure 10 shows the transient current at the left contact ($x = 0$). As we switch at time $t = 0$ out of the equilibrium state ($j = 0$), we can observe that the current suffers one oscillation before achieving its equilibrium state at the valley. Oscillations were also reported in [37] for example where a transient Schrödinger Poisson model was used for the simulation. The current was highly oscillatory because of the ballistic effects. Here, because of the diffusion effects, we cannot expect the same behaviour. Note that the behaviour of the eQDD model is again qualitatively similar to the DG model, the same phenomenon having been reported in [28].

	λ_1	λ_2	λ_3	λ_4	λ_5	λ_6	λ_7
Peak	0.87	1.05	1.56	2.03	2.28	3.03	4.47
Valley	0.87	1.11	1.57	1.70	2.54	3.05	5.03

Table 2
Eigenvalues (Energies [eV]) of the modified Hamiltonian $H[A]$ at the Peak and at the Valley.

4.2.2 Comparison between the eQDD model and the DG model

In Figure 11, we show the results obtained with the Density Gradient model using the same parameters as defined for the eQDD model. As we can see, results are qualitatively similar but differ significantly even if the fourth power of the scaled Planck constant β^4 is between 10^{-6} and 10^{-4} depending on the value of the effective mass. The current is much smaller for the DG model and the peak-to-valley ratios are more important. This may be due to the fact that the heterojunctions of the RTDs create discontinuities not only on the external potential, but also on the quantum chemical potential and so the error estimate made in (26) may not be valid because the quantum chemical potential is not a smooth function. This is not surprising then that these two models give different results on such a device. Even with a smoother external potential (replacing the two step functions by two gaussians), it appears that the current-voltage characteristics are still different for the two models as suggested by figure 12. In order to avoid any confusion induced by the variable mass (the link between both models having been written for a constant effective mass), we take a mass constant and equal to $0.067 \times me$. A parameter which seems important for the models to fit is the height of the double barriers. Indeed, even with a smooth external potential, if the height of the

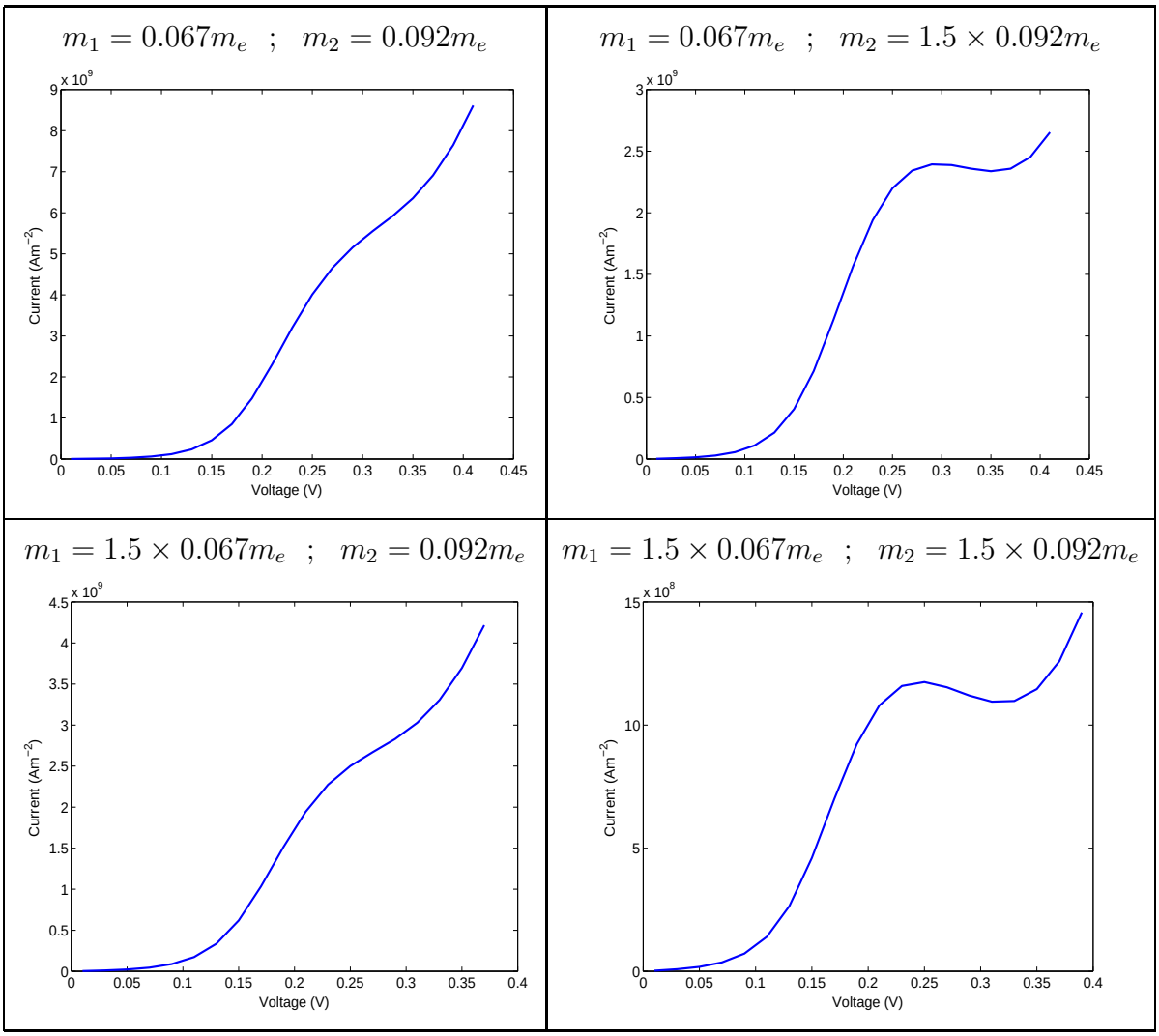

Fig. 6. Influence of the effective mass on the IV curve, m_1 being the mass outside the barriers, and m_2 being the mass inside.

barriers is important, it appears that the density varies a lot, creating a Bohm potential which is not small (in β^2) as needed for the error estimate (27) to be valid.

We have observed that we can fit the results obtained with the eQDD model and the DG model dividing the effective mass (which is equivalent to multiplying the Bohm potential) by an appropriate constant in the DG model. Astonishingly, not only the stationary current fits but also the time behaviour of the density and the current, but we do not yet explain this fact which does not seem to be a coincidence. Moreover, we have not found any convincing physical explanation for this similarity. To finish, figure 13 shows the role of the temperature on the current for an applied bias of $0.2V$ and for the three models eQDD, DG and CDD with a constant mass equal to $0.067m_e$. For fairly large temperatures, the currents seem to converge to the same limit, due to

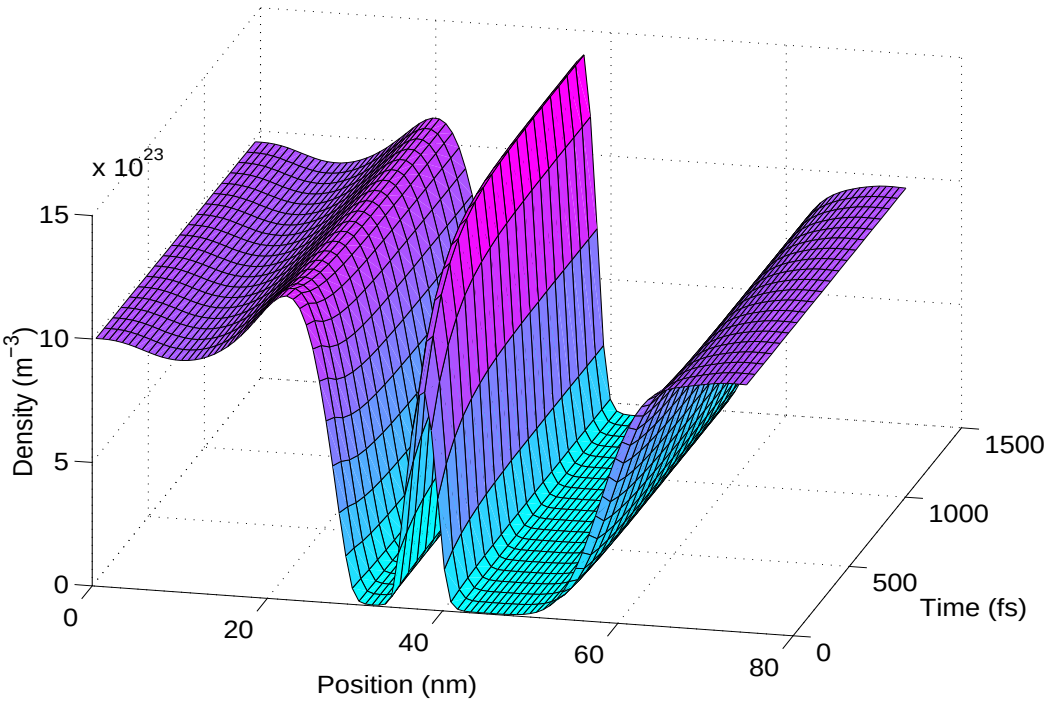

Fig. 7. Evolution of the density from the peak (applied bias: 0.25V) to the valley (applied bias: 0.31V).

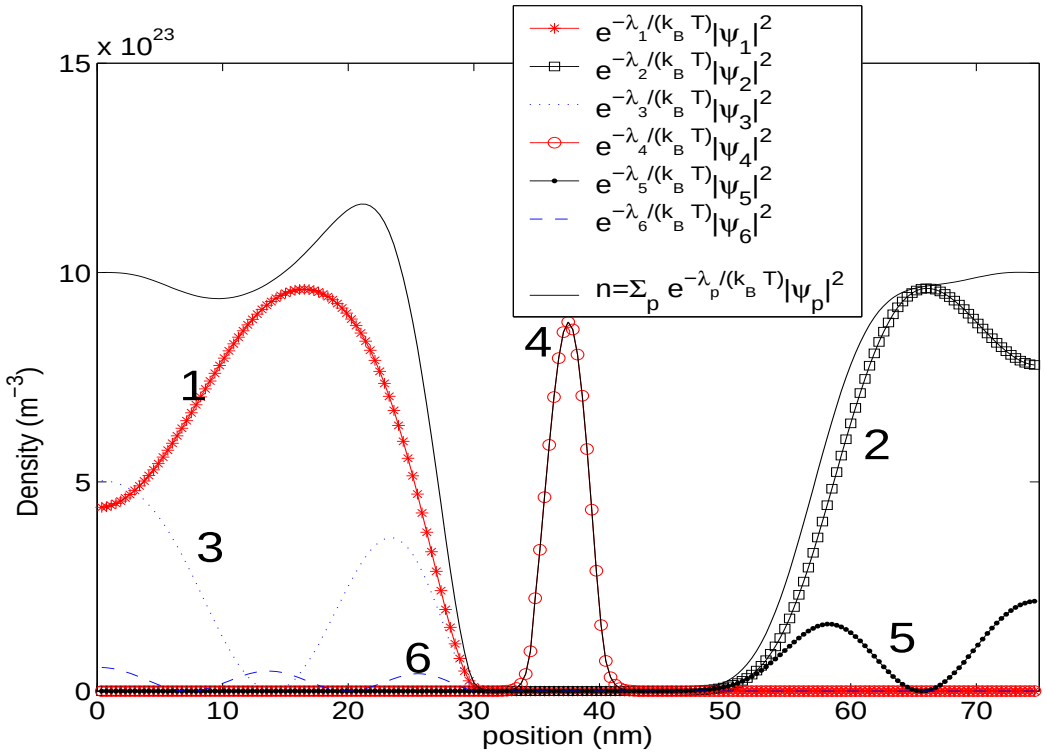

Fig. 8. Density at the peak (Applied bias: 0.25V).

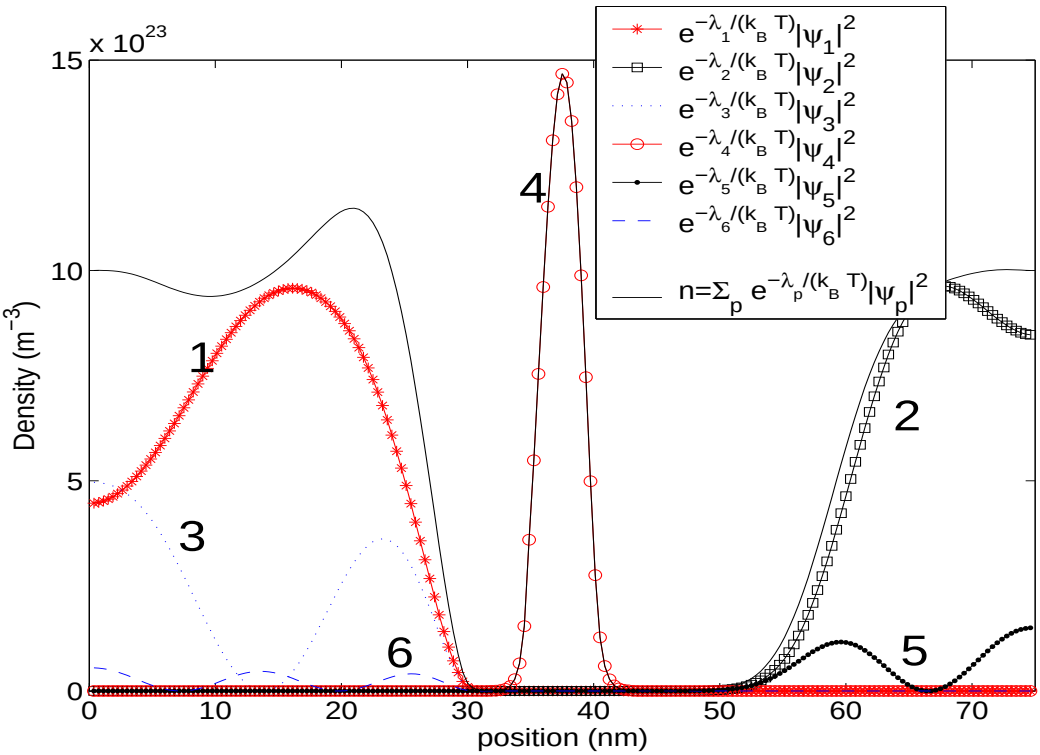

Fig. 9. Density at the valley (Applied bias: 0.31V).

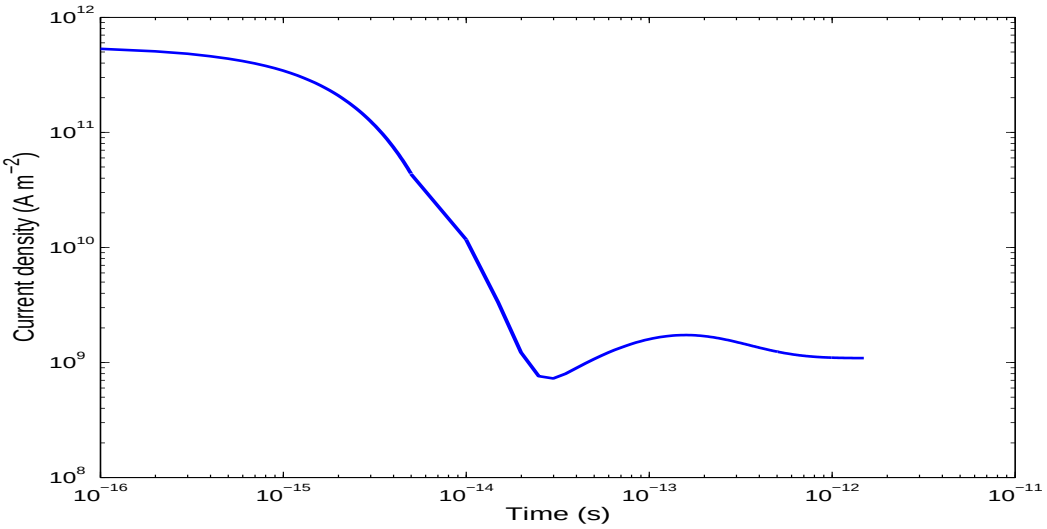

Fig. 10. Transient Current density.

the high thermoionic effects. Moreover, the DG model seems closer from the eQDD model than from the CDD model as discussed in section 2.2 (note that β is small when T is large).

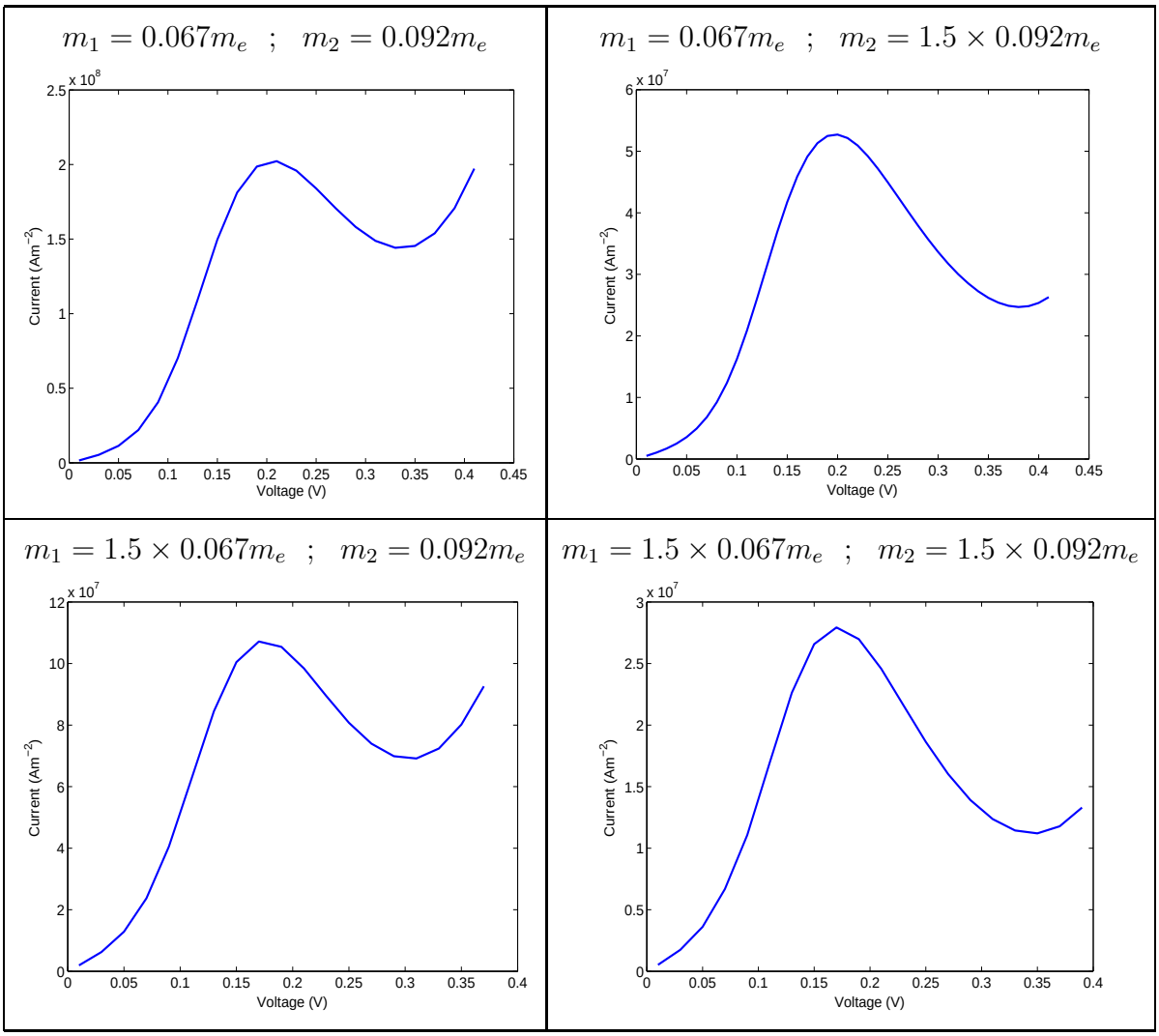

Fig. 11. IV curves obtained with the DG model (m_1 being the mass outside the barriers, and m_2 being the mass inside).

5 Summary and Conclusion

An entropic Quantum Drift-Diffusion model for transport in nanostructures has been presented on a bounded domain. A discretization has been proposed and numerical results have permitted to check the main properties of the model such as entropy dissipation, mass conservation, and convergence to the stationary Schrödinger-Poisson model. The eQDD model captures also some interesting features of the resonant tunneling diode, such as the resonance peak on the IV curve, characteristic of such a device. The model seems to be quite sensitive to the value of the effective mass inside the double barrier. The eQDD model has also been compared to the Schrödinger Poisson Drift Diffusion model on the one hand and the Density Gradient model on the other hand, showing interesting differences: The eQDD model is very close

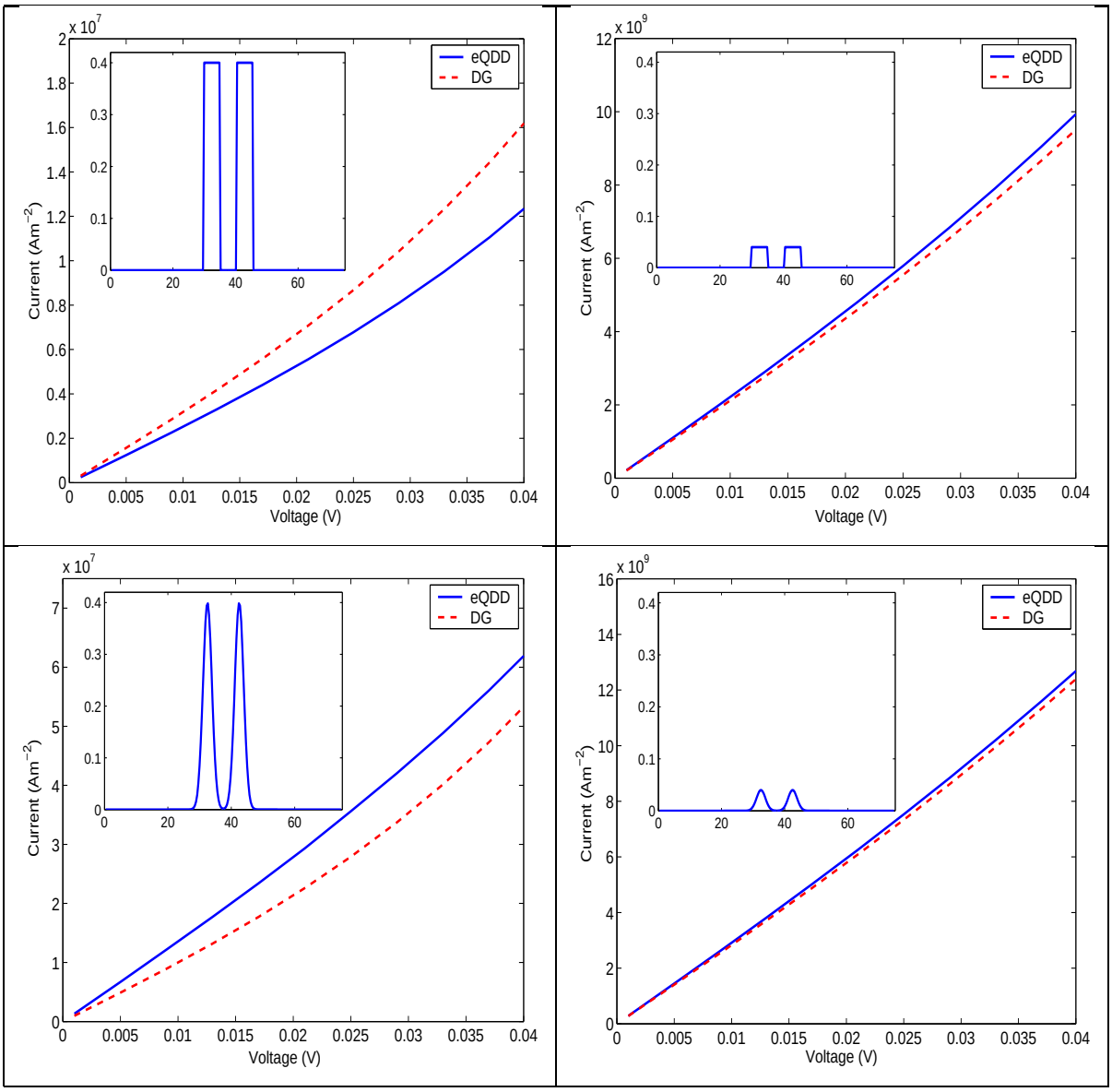

Fig. 12. Influence of the shape and the height of the double barrier on the Current-Voltage characteristics for the eQDD and DG models.

to the SPDD model near the equilibrium but seem to be more stable far from the equilibrium (this is probably because it dissipates free energy). For quantum devices such as RTDs with heterojunctions, the eQDD model and the DG model are not so close quantitatively because of the discontinuity of the potentials but they exhibit similar qualitative behaviour. In a near future, we should incorporate in the eQDD model the continuous spectrum of the modified Hamiltonian H by considering transparent boundary conditions for the wave functions, adapting the work done for the Schrödinger equation in [7, 3, 2, 37, 30].

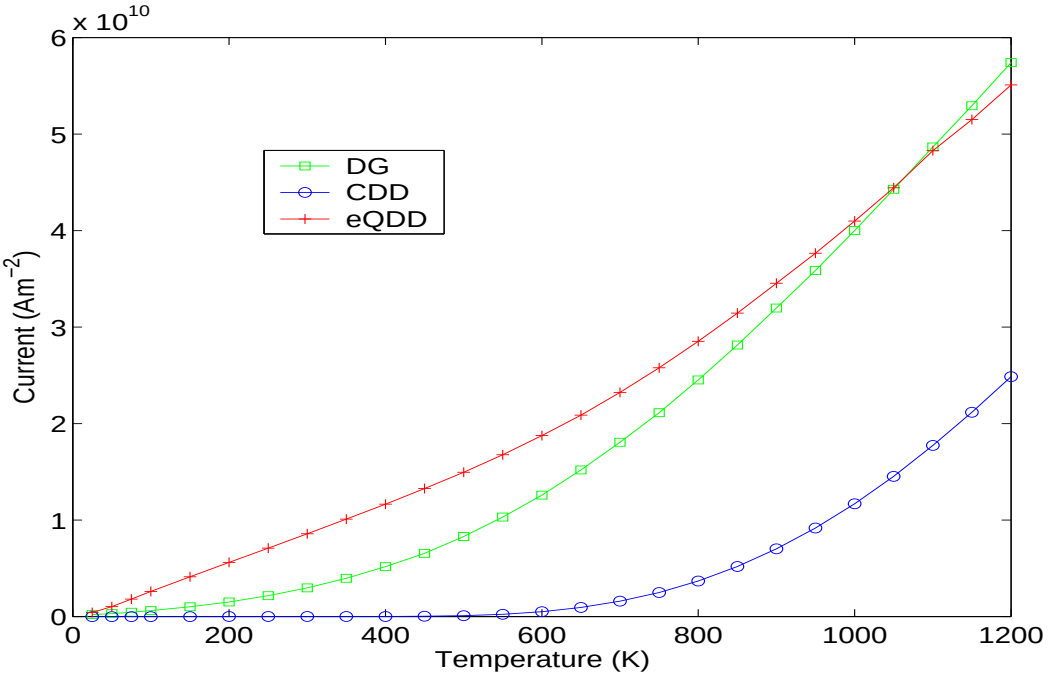

Fig. 13. Current-Temperature curve (applied bias: $0.2V$).

Acknowledgments. Supported by the European network HYKE, funded by the EC as contract HPRN-CT-2002-00282. This work was also supported by the ACI Nouvelles Interfaces des Mathématiques no. ACINIM 176-2004 "MOQUA" and by the ACI Jeunes chercheurs no. JC1035, both funded by the French ministry of research.

A Derivation of the eQDD model

In order to understand why this model dissipates quantum entropy, we are going to recall how it can be derived from the Quantum Liouville equation applying a diffusive limit. In article [14], the diffusive limit is performed on the unbounded domain of dimension d ($\mathbb{R}^d$) using the Wigner transform. Here, we adapt this work to derive the eQDD model in the density matrix formulation, which enables to work on a arbitrary set $\Omega \subset \mathbb{R}^d$ (bounded or not) with a characteristic size L. For the sake of simplicity we are going to suppose that the effective mass m is constant in Ω, but all the following calculations can be extended to the case of a variable effective mass.

Derivation of the model. A quantum particle system can be described by a density operator ρ which is a positive hermitian, trace-class operator satisfying

the collisional Liouville equation:

$$i\hbar\partial_t\rho = [\mathcal{H}, \rho] + i\hbar Q(\rho), \tag{A.1}$$

where $[\mathcal{H}, \rho] = \mathcal{H}\rho - \rho\mathcal{H}$ is the commutator of the Hamiltonian $\mathcal{H} = -\frac{\hbar^2}{2m}\Delta - eV$ and the density operator and $Q(\rho)$ is a collision operator describing the interactions between particles and a thermal bath at temperature T. The density of particles $n(x)$ is defined weakly by:

$$\forall\phi \quad \int_\Omega n(x)\phi(x)dx = \mathrm{Tr}(\rho\phi), \tag{A.2}$$

where on the right hand side, we interpret ϕ as the multiplication operator by the function $\phi(x)$. In order to define this collision operator, we have to introduce the quantum free energy and the Quantum Maxwellians. The microscopic quantum free energy of a system is defined by:

$$G[\rho] = E[\rho] - TS[\rho], \tag{A.3}$$

where E is the energy of the system and S is the quantum entropy. The entropy is given by:

$$S[\rho] = -k_B\mathrm{Tr}(\rho\log\rho), \tag{A.4}$$

and the energy is defined by:

$$E[\rho] = \mathrm{Tr}(\rho\mathcal{H}). \tag{A.5}$$

We obtain the following expression for the microscopic quantum free energy:

$$G[\rho] = \mathrm{Tr}\left(\rho k_B T(\log\rho + \frac{\mathcal{H}}{k_B T})\right). \tag{A.6}$$

Now, we consider the problem of minimizing the quantum free energy G under the constraint of given density $n(x)$:

$$\min\{G[\rho] \mid \forall\phi \quad \int n(x)\phi(x)dx = \mathrm{Tr}(\rho\phi)\}. \tag{A.7}$$

Assuming that this minimization problem has a solution, this solution is given by [17, 14]:

$$\rho[A] = \exp(-\frac{H[A]}{k_B T}),$$

where $H[A]$ is the modified Hamiltonian defined in relation (4) and $A = A(x)$ is a quantum chemical potential which is determined in such a way that the density constraint in (A.7) is satisfied. We note $\mathcal{M}_\rho = \exp(-\frac{H[A]}{k_B T})$ the quantum Maxwellian which has the same density as ρ (*i.e* $\mathrm{Tr}(\mathcal{M}_\rho\phi) = \mathrm{Tr}(\rho\phi)\ \forall\phi$). Now, we define the collision operator as follows:

$$Q(\rho) = \frac{\mathcal{M}_\rho - \rho}{\tau}. \tag{A.8}$$

where τ is the relaxation time of the collision operator which can be found from the mobility of the material: $\tau = \frac{m\mu}{e}$. We expect that, as in the classical setting, this simple collision operator of BGK type provides a simple relaxation model with similar features as physically more realistic operators. Now we want to perform a diffusive limit on the quantum Liouville equation. For this purpose, we start by doing the same scaling as in section 2.1.2 on the quantum Liouville equation and we obtain (omitting the primes):

$$i\varepsilon\partial_t\rho^\varepsilon = \frac{1}{\sqrt{2}\beta}[\mathcal{H}, \rho^\varepsilon] + i\frac{\mathcal{M}_{\rho^\varepsilon} - \rho^\varepsilon}{\varepsilon}, \tag{A.9}$$

where $\mathcal{H} = -\beta^2\Delta + V$. The dimensionless parameter β is the scaled Planck constant and the dimensionless parameter ε is the scaled mean free path defined by:

$$\varepsilon = \sqrt{\frac{k_B T}{m}}\frac{\tau}{L} = \frac{\lambda_{\text{mfp}}}{L}.$$

A typical value of ε is $\varepsilon \sim 0.5$ at $T \sim 77K$. In smaller temperatures, ε can be estimated to be small and the limit $\varepsilon \to 0$ can be investigated. Even if ε is not small, the limit $\varepsilon \to 0$ can be believed to at least provides a reasonable approximation of the problem.

Therefore, we are interested in the limit $\varepsilon \to 0$. We assume that $\rho^\varepsilon \to \rho^0$ as $\varepsilon \to 0$. Then at leading order, we have $Q(\rho^0) = 0$ which means that ρ^0 belongs to the null space of the collision operator Q. Thus, we deduce that there exists a function $A(x,t)$ such that

$$\rho^0 = e^{-H[A]}, \tag{A.10}$$

with $H[A]$ the modified scaled Hamiltonian:

$$H[A] = -\beta^2\Delta + A.$$

Now we introduce the following Chapman-Enskog expansion:

$$\rho^\varepsilon = \mathcal{M}_{\rho^\varepsilon} + \varepsilon\rho_1^\varepsilon. \tag{A.11}$$

Then, clearly:

$$\frac{\mathcal{M}_{\rho^\varepsilon} - \rho^\varepsilon}{\varepsilon} = -\rho_1^\varepsilon.$$

Inserting this expression into equation (A.9) and taking the limit $\varepsilon \to 0$ we get:

$$\rho_1^0 = -\frac{i}{\sqrt{2}\beta}[\mathcal{H}, \rho^0]. \tag{A.12}$$

Now, we compose equation (A.9) with the multiplication by a test function ϕ and we take the trace. We use that, by definition, $\text{Tr}((\mathcal{M}_\rho - \rho)\phi) = 0$ and we get:

$$\text{Tr}(i\partial_t\rho^\varepsilon\phi) - \frac{1}{\sqrt{2}\beta\varepsilon}\text{Tr}([\mathcal{H}, \rho^\varepsilon]\phi) = 0. \tag{A.13}$$

We can simplify this equation by noticing that:

$$\mathrm{Tr}([\mathcal{H}, \mathcal{M}_{\rho^\varepsilon}]\phi) = 0.$$

Indeed, $\mathcal{H} = H[A^\varepsilon] - (A^\varepsilon - V)$ where A^ε is such that $\mathcal{M}_{\rho^\varepsilon} = e^{-H[A^\varepsilon]}$, so that $[\mathcal{H}, \mathcal{M}_{\rho^\varepsilon}] = [H[A^\varepsilon], \mathcal{M}_{\rho^\varepsilon}] - [A^\varepsilon - V, \mathcal{M}_{\rho^\varepsilon}]$. The first commutator is equal to zero because the commutator between an operator and its exponential is zero. The trace of the second commutator multiplied by ϕ is equal to zero because of the cyclicity of the trace. We remind that $\forall(a, b, c)$, we have $\mathrm{Tr}([a, b]c) = \mathrm{Tr}(a[b, c]) = \mathrm{Tr}([c, a]b)$ so that $\mathrm{Tr}([A^\varepsilon - V, \mathcal{M}_{\rho^\varepsilon}]\phi) = \mathrm{Tr}([\phi, A^\varepsilon - V]\mathcal{M}_{\rho^\varepsilon}) = 0$ (ϕ and $A^\varepsilon - V$ being operators of multiplication by functions). Equation (A.13) becomes:

$$\mathrm{Tr}(i\partial_t \rho^\varepsilon \phi) - \frac{1}{\sqrt{2}\beta}\mathrm{Tr}([\mathcal{H}, \rho_1^\varepsilon]\phi) = 0$$

At the limit $\varepsilon \to 0$ and using (A.12), we obtain:

$$\mathrm{Tr}(i\partial_t \rho^0 \phi) + \frac{1}{2\beta^2}\mathrm{Tr}(i[\mathcal{H}, [\mathcal{H}, \rho^0]]\phi) = 0.$$

We again use the fact that the commutator between an operator and its exponential is zero, so

$$[\mathcal{H}, \rho^0] = -[A - V, \rho^0].$$

Also using the cyclicity of the trace, we find that $\mathrm{Tr}([\mathcal{H}, [A - V, \rho^0]]\phi) = \mathrm{Tr}([-\beta^2\Delta, [A - V, \rho^0]]\phi)$ and we obtain:

$$\mathrm{Tr}(i\partial_t \rho^0 \phi) - \frac{1}{2\beta^2}\mathrm{Tr}(i[-\beta^2\Delta, [A - V, \rho^0]]\phi) = 0.$$

Now, we can prove that

$$\mathrm{Tr}([-\beta^2\Delta, [A - V, \rho^0]]\phi) = 2\beta^2\mathrm{Tr}(\rho^0 \nabla\phi \cdot \nabla(A - V)).$$

Indeed, using the cyclicity of the trace, we first see that $\mathrm{Tr}([-\Delta, [A-V, \rho^0]]\phi = \mathrm{Tr}(\rho^0[[\Delta, \phi], A - V])$, and second, a direct computation of the double commutator leads to the fact that $[[\Delta, \phi], A - V] = 2\nabla\phi \cdot \nabla(A - V)$. The density being weakly defined by:

$$\forall\phi \quad \int_\Omega n\phi dx = \mathrm{Tr}(\rho^0\phi), \tag{A.14}$$

we finally obtain the following equality being true for every test function ϕ:

$$\int_\Omega (\partial_t n\phi - n\nabla(A - V) \cdot \nabla\phi)dx = 0,$$

which gives after an integration by parts the dimensionless version of the eQDD model (6)-(7) in a weak formulation.

Entropic character of the model. We are now able to prove that the eQDD model dissipates the quantum free energy. The scaled microscopic quantum free energy reads:

$$G(\rho) = \mathrm{Tr}(\rho(\log\rho + \mathcal{H})),$$

so that

$$\frac{d}{dt}G(\rho) = \mathrm{Tr}((\log\rho + \mathcal{H} + \mathrm{Id})\partial_t\rho).$$

This identity is not obvious and uses a formula for the derivative of G with respect to ρ which can be found in [17] or [14]. Using the Liouville equation (A.9), we obtain:

$$\frac{d}{dt}G(\rho^\varepsilon) = \mathrm{Tr}((\log\rho^\varepsilon + \mathcal{H} + \mathrm{Id})(-i\frac{[\mathcal{H},\rho^\varepsilon]}{2\beta^2\varepsilon} + \frac{\mathcal{M}_{\rho^\varepsilon} - \rho^\varepsilon}{2\beta^2\varepsilon^2})).$$

But using the cyclicity of the trace, we find:

$$\mathrm{Tr}((\log\rho^\varepsilon + \mathcal{H} + \mathrm{Id})(-i\frac{[\mathcal{H},\rho^\varepsilon]}{2\beta^2\varepsilon})) = 0,$$

and using the convexity of the quantum free energy, we have the inequality:

$$G'(\rho^\varepsilon)(\mathcal{M}_{\rho^\varepsilon} - \rho^\varepsilon) = \mathrm{Tr}((\log\rho^\varepsilon + \mathcal{H} + \mathrm{Id})(\mathcal{M}_{\rho^\varepsilon} - \rho^\varepsilon)) \leq G(\mathcal{M}_{\rho^\varepsilon}) - G(\rho^\varepsilon).$$

Because $\mathcal{M}_{\rho^\varepsilon}$ is chosen to minimize G, we finally have:

$$\frac{d}{dt}G(\rho^\varepsilon) \leq 0.$$

This inequality is true at the limit $\varepsilon \to 0$, giving the dissipation of the macroscopic quantum free energy:

$$G(n) = \int_\Omega -n(A - V)\ dx.$$

Relation between the density and the quantum chemical potential. Note that if A belongs to $L^2(\Omega)$ and if we choose for $H[A]$ a domain such that $H[A]$ has a compact resolvent (putting Neumann conditions on the wave functions for example), $H[A]$ possesses an orthogonal basis of eigenfunctions $(\psi_p[A])_{p=1\cdots\infty}$ associated with the eigenvalues $\lambda_1[A] \leq \lambda_2[A] \leq ....$ The relation (A.14) between n and A takes a more explicit form:

$$n[A] = \sum_{p\geq 1} \exp(-\lambda_p[A])|\psi_p[A]|^2, \tag{A.15}$$

where the ψ_p are normalized:

$$\int_\Omega \psi_p\psi_q = \delta_{pq}.$$

Indeed, we can write:

$$\begin{aligned}\forall\phi \quad \int_\Omega n\phi \; dx &= \mathrm{Tr}(e^{-H[A]}\phi) \\ &= \sum_{p\geq 1} \left(\phi e^{-H[A]}\psi_p, \psi_p\right)_{L^2(\Omega)} \\ &= \sum_{p\geq 1} \int_\Omega \phi e^{-\lambda_p}|\psi_p|^2 \; dx \\ &= \int_\Omega (\sum_{p\geq 1} e^{-\lambda_p}|\psi_p|^2)\phi \; dx,\end{aligned}$$

defining weakly the density.

B The dimensionless models in dimension 1 with variable parameters

In this section, for the sake of completeness, the dimensionless models with variable mass, permittivity and mobility are written.

The eQDD model. The entropic Quantum Drift-Diffusion model coupled with the Poisson equation is written:

$$\begin{aligned}&\partial_t n + \partial_x j = 0, \\ &j = n\mu(x)\partial_x(A - (V_s + V_{ext})), \\ &-\alpha^2(\partial_x \varepsilon(x)\partial_x V_s) = C - n, \\ &n = \sum_{p\geq 1} e^{-\lambda_p}|\psi_p|^2,\end{aligned}$$

where (λ_p, ψ_p) are the eigenvalues and eigenfunctions of $H[A] = -\beta^2\partial_x(\frac{1}{m(x)}\partial_x) + A$, with α and β the scaled Debye length and the scaled de Broglie length:

$$\begin{aligned}\alpha &= \sqrt{\frac{\overline{\varepsilon} k_B T}{e^2 L^2 \overline{n}}} = \frac{\lambda_D}{L}, \\ \beta &= \sqrt{\frac{\hbar^2}{2\overline{m} L^2 k_B T}} = \frac{\lambda_{dB}}{L}.\end{aligned}$$

The reference values for the mobility $\overline{\mu}$,the effective mass $\overline{m}$ and the permittivity $\overline{\varepsilon}$ are chosen as follows:

$$\overline{\mu} = \max|\mu(x)| \quad ; \quad \overline{m} = \max|m(x)| \quad ; \quad \overline{\varepsilon} = \max|\varepsilon(x)|$$

The DG model and the CDD model. The Density Gradient model coupled with the Poisson equation is written:

$$
\begin{aligned}
&\partial_t n + \partial_x j = 0,\\
&j = n\mu(x)\partial_x(-\log n - (V_s + V_{ext} + V^B)) = 0,\\
&-\alpha^2\partial_x(\varepsilon(x)\partial_x V_s) = n - C,\\
&V_B = -\frac{\beta^2}{3}\frac{\partial_x(\frac{1}{m}\partial_x\sqrt{n})}{\sqrt{n}}.
\end{aligned}
$$

For the Classical Drift-Diffusion model, we take $V_B = 0$.

The SPDD model. The Schrödinger-Poisson Drift-Diffusion model coupled with the Poisson equation is written:

$$
\begin{aligned}
&\partial_t n + \partial_x j = 0,\\
&j = n\mu(x)\partial_x(A - (V_s + V_{ext})) = 0,\\
&-\alpha^2\partial_x\varepsilon(x)\partial_x V_s = C - n,\\
&n = \sum_{p\geq 1} e^{-\lambda_p - A + (V_s + V_{ext})}|\psi_p|^2,
\end{aligned}
$$

where (λ_p, ψ_p) are the eigenvalues and eigenfunctions of the Hamiltonian $\mathcal{H} = H[V_s + V_{ext}] = -\beta^2\partial_x(\frac{1}{m(x)}\partial_x) + (V_s + V_{ext})$.

References

[1] N. Ben Abdallah. A hybrid kinetic-quantum model for stationary electron transport in a resonant tunneling diode. *J. Stat. Phys.*, 90:627–662, 1998.

[2] N. Ben Abdallah. On a multidimensional schrödinger-poisson scattering model for semiconductors. *J. Math. Phys.*, 41:4241–4261, 2000.

[3] N. Ben Abdallah, P. Degond, and P. A. Markowich. On a one-dimensional schrödinger-poisson scattering model. *Z. Angew. Math. Phys.*, 48:135–155, 1997.

[4] N. Ben Abdallah and A. Unterreiter. On the stationary quantum drift-diffusion model. *Z. Angew. Math. Phys.*, 49(2):251–275, 1998.

[5] M. G. Ancona and G. J. Iafrate. Quantum correction of the equation of state of an electron gas in a semiconductor. *Phys. review*, B 39:9536–9540, 1989.

[6] M. G. Ancona and H. F. Tiersten. Macroscopic physics of the silicon inversion layer. *Pys. review*, B 39:7959–7965, 1987.

[7] A. Arnold. Mathematical concepts of open boundary conditions. *Phys. Lett.*, 30:561–584, 2001.

[8] A. Arnold and F. Nier. The two-dimensional wigner-poisson problem for an electron gas in the charge neutral case. *Math. Methods Appl. Sci.*, 14(9):595–613, 1991.

[9] M. Baro, N. Ben Abdallah, P. Degond, and A. El Ayyadi. A 1d coupled schrödinger drift-diffusion model including collisions. *J. Comput. Phys.*, 203:129–153, 2005.

[10] L. L. Chang, L. Esaki, and R. Tsu. Resonant tunneling in semiconductor double barriers. *Appl. Phys. Lett.*, 24:593–595, 1974.

[11] R.-C. Chen and J.-L. Liu. A quantum corrected energy-transport model for nanoscale semiconductor devices. *J. Comput. Phys.*, 204:131–156, 2005.

[12] C. de Falco, E. Gatti, A. L. Lacaita, and R. Sacco. Quantum-corrected drift-diffusion models for transport in semiconductor devices. *J. Comput. Phys.*, 204(2):533–561, 2005.

[13] P. Degond and A. El Ayyadi. A coupled schrödinger drift-diffusion model for quantum semiconductor devices. *J. Comput. Phys.*, 181:222–259, 2002.

[14] P. Degond, F. Méhats, and C. Ringhofer. Quantum energy-transport and drift-diffusion models. *J. Stat. Phys.*, 118(3/4), 2005.

[15] P. Degond, F. Méhats, and C. Ringhofer. Quantum hydrodynamic models derived from the entropy principle. *Contemporary Mathematics*, 371, 2005.

[16] P. Degond and C. Ringhofer. Binary quantum collision operators conserving mass momentum and energy. *C. R. Acad. Sci. Paris*, I 336(9):785–790, 2003.

[17] P. Degond and C. Ringhofer. Quantum moment hydrodynamics and the entropy principle. *J. Stat. Phys.*, 112(314):587–628, August 2003.

[18] S. Gallego and F. Méhats. Numerical approximation of a quantum drift-diffusion model. *C. R. Acad. Sci. Paris*, Ser I 339:519–524, 2004.

[19] S. Gallego and F. Méhats. Entropic discretization of a quantum drift-diffusion model. To appear in SIAM journal on numerical analysis, 2005.

[20] C. Gardner. The quantum hydrodynamic model for semiconductor devices. *SIAM J. Appl. Math.*, 54(2):409–427, 1994.

[21] C. Gardner and C. Ringhofer. The smooth quantum potential for the hydrodynamic model. *Phys. Rev.*, E 53:157–167, 1996.

[22] C. Gardner and C. Ringhofer. The chapman-enskog expansion and the quantum hydrodynamic model for semiconductor devices. *VLSI Design*, 10:415–435, 2000.

[23] I. Gasser and A. Jüngel. The quantum hydrodynamic model for semiconductors in thermal equilibrium. *Z. Angew. Math. Phys.*, 48(1):45–59, 1997.

[24] I. Gasser and P. A. Markowich. Quantum hydrodynamics, wigner transforms and the classical limit. *Asympt. Analysis*, 14(2):97–116, 1997.

[25] I. Gasser, P. A. Markowich, and C. Ringhofer. Closure conditions for classical and quantum moment hierarchies in the small temperature limit.

Transp. Th. Stat. Phys, 25(3-5):409–423, 1996.

[26] A. Jüngel. *Quasi-hydrodynamic semiconductor equations, Progress in Nonlinear Differential Equations*. Birkhuser, 2001.

[27] A. Jüngel and A. El Ayyadi. Semiconductor simulations using a coupled quantum drift-diffusion schrödinger-poisson model. To appear in SIAM J. Appl. Math., 2005.

[28] A. Jüngel and R. Pinnau. A positivity preserving numerical scheme for a fourth order parabolic equation. *SIAM J. Num. Anal.*, 39(2):385–406, 2001.

[29] N. C. Kluksdahl, A. M. Kriman, D. K. Ferry, and C. Ringhofer. Self-consistent study of the resonant-tunneling diode. *Phys. Rev.*, B39:7720–7735, 1989.

[30] C. S. Lent and D. J. Kirkner. The quantum transmitting boundary method. *J. Appl. Phys.*, 67:6353–6359, 1990.

[31] C. D. Levermore. Moment closure hierarchies for kinetic theories. *J. Stat. Phys*, 83:1021–1065, 1996.

[32] P. A. Markowich, C. Ringhofer, and C. Schmeiser. *Semiconductor Equations*. Springer, 1990.

[33] S. Micheletti, R. Sacco, and P. Simioni. Numerical simulation of resonant tunnelling diodes with a quantum-drift-diffusion model. *Scientific Computing in Electrical Engineering, Lecture Notes in Computer Science, Springer-Verlag*, pages 313–321, 2004.

[34] P. Mounaix, O. Vanbésien, and D. Lippens. Effect of cathode spacer layer on the current voltage characteristics of resonant tunneling diodes. *App. Phys. Let.*, 2(5):489–510, 1990.

[35] F. Nier. A stationary schrödinger-poisson system arising from the modelling of electronic devices. *Forum Math.*, 2(5):489–510, 1990.

[36] F. Nier. A variational formulation of schrödinger-poisson systems in dimension $d \leq 3$. *Comm. Partial Differential Equations*, 18(7-8):1125–1147, 1993.

[37] O. Pinaud. Transient simulations of a resonant tunneling diode. *J. Appl. Phys.*, 92(4):1987–1994, 2002.

[38] A. Pirovano, A. Lacaita, and A. Spinelli. Two-dimensional quantum effects in nanoscale mosfets. *IEEE Trans Electron Devices*, 47:25–31, 2002.

[39] E. Polizzi and N. Ben Abdallah. Self-consistent three dimensional models for quantum ballistic transport in open systems. *Phys. Rev.*, B 66, 2002.

[40] S. Teufel. *Adiabatic Perturbation Theory in Quantum Dynamics*. Springer-Verlag, 2003.

[41] A. Unterreiter and R. Pinnau. The stationary current-voltage characteristics of the quantum drift-diffusion model. *SIAM J. Num. Anal.*, 37(1):211–245, 1999.